Received 19 January 2018; revised 14 March 2018; accepted 23 March 2018. Date of publication 27 March 2018;
date of current version 27 June 2018. The review of this paper was arranged by Editor A. Nathan.

Digital Object Identifier 10.1109/JEDS.2018.2820003

Effect of Al_2O_3 Passivation Layer and Cu Electrodes on High Mobility of Amorphous IZO TFT

SHIBEN HU [1], HONGLONG NING [1], KUANKUAN LU [1], ZHIQIANG FANG [2], RUIQIANG TAO [1], RIHUI YAO [1], JIANHUA ZOU [1], MIAO XU [1], LEI WANG [1], AND JUNBIAO PENG [1]

1 Institute of Polymer Optoelectronic Materials and Devices, State Key Laboratory of Luminescent Materials and Devices, South China University of Technology, Guangzhou 510640, China
2 State Key Laboratory of Pulp and Paper Engineering, South China University of Technology, Guangzhou 510640, China

CORRESPONDING AUTHORS: H. NING AND R. YAO (e-mail: ninghl@scut.edu.cn; yaorihui@scut.edu.cn)

This work was supported in part by the National Key Research and Development Program of China under Grant 2016YFB0401504, in part by the National Natural Science Foundation of China under 51771074 and Grant U1601651, in part by the National Key Basic Research and Development Program of China (973 Program) under Grant 2015CB655004, in part by MOST, Science and Technology Project of Guangdong Province under Grant 2016B090907001, Grant 2016A040403037, and Grant 2015B090914003, and in part by the Guangdong Natural Science Foundation under Grant 2016A030313459.

ABSTRACT In this paper, we present a high mobility amorphous indium–zinc–oxide (a-IZO) thin film transistor (TFT) based on copper (Cu) source/drain electrodes (S/D) and aluminum oxide (Al_2O_3) passivation layer (PVL). The mechanism of high mobility for the a-IZO TFT based on Cu S/D with Al_2O_3 PVL was proposed and experimentally demonstrated. The sputtering of Al_2O_3 PVL induced a highly conductive channel layer due to the formation of In-rich layer on the back channel. Also, Cu S/D presented Schottky contact behavior compared with Mo S/D which behaved like Ohmic contact. Because the Schottky contact can block leakage current and the highly conductive channel achieved high on-current, the a-IZO TFT based on Cu S/D and Al_2O_3 PVL performed remarkable saturation mobility up to 412.7 cm^2/Vs. This paper presents a feasible way to implement high mobility TFT arrays with Cu electrodes.

INDEX TERMS Copper, aluminum oxide, a-IZO, Schottky contact, mobility.

I. INTRODUCTION

As display technology advances in size, resolution, and refresh rate, high mobility thin film transistor (TFT) arrays with low resistance electrodes are needed to improve the RC delay to avoid signal distortion [1]–[5]. Amorphous oxide semiconductor TFTs have attracted considerable attention on flat panel display backplanes because of their high mobility and excellent uniformity [6]. On the other hand, copper (Cu) is considered an appropriate electrode material for its lower resistivity than aluminum (Al). Although TFTs with mobilities in excess of 100 cm^2/Vs have been implemented, these TFTs do not involve Cu electrodes [7]–[10].

In this paper, we employed aluminum oxide (Al_2O_3) to passivate the amorphous indium-zinc-oxide (a-IZO) TFT with Cu source/drain electrodes (S/D). The introduction of Al_2O_3 PVL significantly improved the conductivity of a-IZO channel layer. Also, the Cu S/D formed a Schottky contact with the channel layer, which made the a-IZO TFT exhibited typical switching characteristics. In a combination of these two effects, the a-IZO TFT achieves a saturation mobility as high as 412.7 cm^2/Vs.

II. EXPERIMENTS

The a-IZO TFTs were prepared with a bottom-gate, top-contact configuration. Firstly, an Al gate electrode was deposited on the glass with a thickness of 300 nm. Then, an anodic Al_2O_3 gate insulator layer having a thickness of 200 nm was constituted on the surface of the gate electrode by anodic oxidation process. The details of anodic oxidation technology have ever been reported elsewhere [11]. Then, a 25-nm thick a-IZO (In: Zn=1:1, at. %) film was deposited by RF magnetron sputtering and patterned through a metal shadow mask. The sputtering process was carried out in Ar/O_2 atmosphere (100/5) at the pressure of 1 mTorr and the sputtering power of 80 W at room temperature. Cu or Mo thin films (100 nm of thickness), as source and

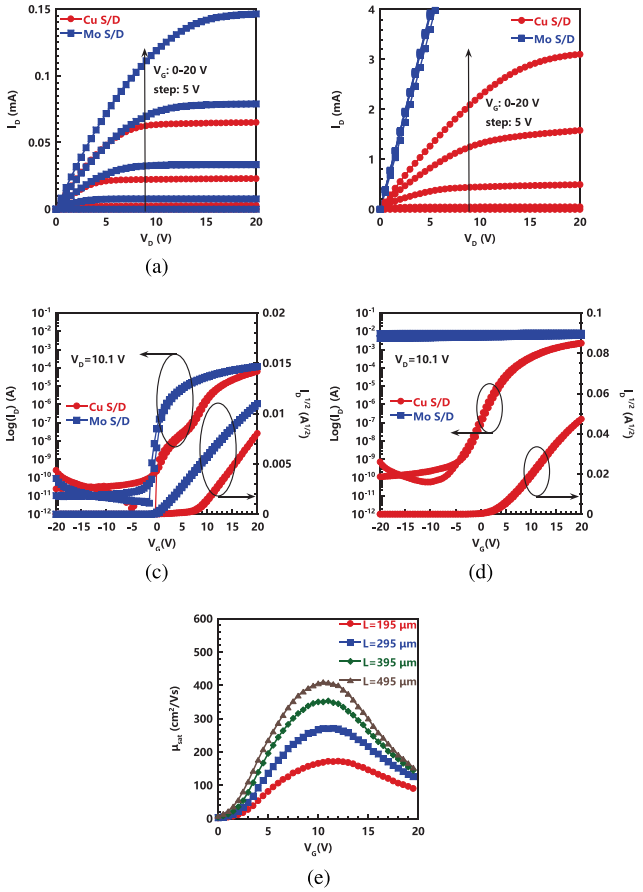

FIGURE 1. **Output characteristics of the (a) non-passivated and (b) passivated TFTs; Transfer characteristics of the (c) non-passivated and (d) passivated TFTs; (e) Dependence of channel length (L) on the Mobility (μ_{sat}) of the passivated Cu-contact TFT.**

drain electrodes (S/D), were deposited on an a-IZO layer by DC magnetron sputtering and patterned using a shadow mask (the sputtering power was 100 W, the pressure was 2 mTorr). The device channel width (W) and length (L) were 625 μm and 495 μm, respectively. After that, a 100-nm thick Al_2O_3 film, as a passivation layer (PVL), was formed by RF magnetron sputtering (the sputtering power was 120 W, the pressure was 1 mTorr). Finally, a thermal treatment was carried out in an argon atmosphere at 300 °C for 1 hour.

The cross-sectional properties of each functional films were characterized by transmission electron microscopy (TEM, FEI HELIOS NANOLAB 450s) equipped with an X-ray energy-dispersive spectroscopy (EDS). The electrical characterization was conducted by a semiconductor parameter analyzer (Agilent 4155C) in the air.

III. RESULTS AND DISCUSSIONS

Four kinds of a-IZO TFTs were prepared, including non-passivated Cu-contact TFT, non-passivated Mo-contact TFT, passivated Cu-contact TFT and passivated Mo-contact TFT. Fig. 1 shows representative output and transfer curves of the above four TFTs. Moreover, electrical performance of the four TFTs is summarized in Table 1. The saturation mobility

TABLE 1. **Comparison of the performance for both a-IZO TFTs.**

S/D	Al_2O_3 PVL	V_{th} (V)	μ_{sat} (cm^2/Vs)	SS (V/dec)	I_{on}/I_{off}
Cu	No	8.0	18.6	0.9	7.3×10^6
Mo	No	0.5	15.9	0.2	3.0×10^7
Cu	Yes	3.6	412.7	1.5	3.9×10^7
Mo	Yes	—	—	—	—

(μ_{sat}), and the threshold voltage (V_{th}) were obtained from the curve of $I_D^{1/2}$ versus the V_G in saturated operation region:

$$I_D^{1/2} = \left(\frac{WC_i\mu_{sat}}{2L}\right)^{1/2}(V_G - V_{th}) \quad (1)$$

Here, C_i is the gate capacitance per unit area of the insulator layer. Moreover, the subthreshold swing (SS) was extracted as the inverse of the maximum slope of the curve of Log I_D versus the V_G [12]:

$$SS = \left[\left(\frac{dLogI_D}{dV_G}\right)_{max}\right]^{-1} \quad (2)$$

Without passivation, both devices exhibit standard switching characteristics. We note that output current of the Cu-contact device is significantly lower than that of the Mo-contact device. This effect may be due to the higher series resistance between Cu and a-IZO than between Mo and a-IZO. Meanwhile, the Cu-contact device shows significant performance degradation, such as hump behavior, relatively positive V_{th} and large SS. It is a common phenomenon in many reports due to the diffusion of Cu caused by the thermal treatment [13]. With passivation, the output current of the TFTs sharply increases that the Mo-contact TFT exceeds 10 mA and the Cu-contact TFT reaches up to 3.1 mA. This increase implies that a highly conductive channel formed between the S and D electrodes induced by the passivation layer. Interestingly, the Mo-contact TFT shows conductor behavior that the output curve is linear, and the gate voltage could not modulate the drain current. Furthermore, the Cu-contact TFTs achieves improved performance as follows: V_{th} of 3.6 V, μ_{sat} of 412.7 cm^2/Vs, SS of 1.5 V/dec and I_{on}/I_{off} ratio of 3.9×10^7. Moreover, the dependence of the channel length on the mobility of the passivated Cu-contact TFT is then investigated. As the channel length reduces from 495 μm to 195 μm, the μ_{sat} decreases from 412.7 cm^2/Vs to 172.2 cm^2/Vs. This effect might be ascribed to the existence of relatively high contact resistance. Due to the significant decrease in channel resistance, the voltage across the channel will substantially decrease, thereby underestimating the true mobility. Therefore, we can conclude that Al_2O_3 PVL and Cu S/D play essential roles in the high mobility of the passivated Cu-contact device.

For evaluating the effect of Cu S/D and Al_2O_3 PVL, transmission line method (TLM) [14] was utilized to trace the variation of the channel and contact resistance using TFTs with different channel length. The total resistance (R_T) was defined as the sum of channel resistance (R_{ch}) and contact

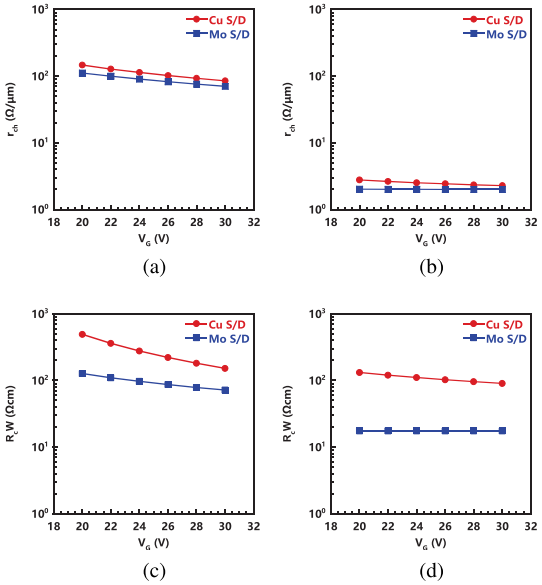

FIGURE 2. Channel resistance per unit channel length (r_{ch}) of the (a) non-passivated and (b) passivated TFTs; Contact resistance (R_C) of the (c) non-passivated and (d) passivated TFTs.

resistance (R_C) at $V_D = 0.1$ V:

$$R_T = \frac{V_D}{I_D} = R_{ch} + R_C = r_{ch}L + R_C \tag{3}$$

Here, r_{ch} is the channel resistance per unit channel length. Fig. 2 exhibits the variation of r_{ch} and R_C values of the a-IZO TFTs. It is observed that r_{ch} of the passivated TFTs significantly decreases about two orders of magnitude compared with that of the non-passivated TFTs. The decrease of r_{ch} confirms that the sputtering of Al_2O_3 PVL can dramatically reduce the channel resistance in a-IZO TFTs. Compared with the two Mo-contact TFTs, R_C of the two Cu-contact TFTs significantly increases. This increase is consistent with the previous report that Cu diffusion leads to a decrease in carrier concentration beneath the S/D, inducing an increase in contact resistance [15]. Finally, we note that the passivated Mo-contact TFT has the similar r_{ch} and lower R_C as the passivated Cu-contact TFT. However, the passivated Mo-contact TFT behaves like a conductor and the passivated Cu-contact TFT exhibits typical switching characteristic. So, switching property of the Cu-contact device should be a result of the high contact resistance by Cu S/D. Based on their electrical properties, we can attribute the high mobility of the passivated Cu-contact a-IZO TFT to high contact resistance caused by Cu S/D and low channel resistance due to Al_2O_3 sputtering.

Cross-sectional scanning transmission electron microscopy (STEM) integrated with X-ray energy dispersive spectroscopy (EDS) was used to clarify the interface reaction of Al_2O_3 PVL with the a-IZO channel layer. Fig. 3(a) displays a cross-sectional STEM image of the Cu-contact TFT channel, while fig. 3(b) shows a magnified STEM image taken from the interface. Interfacial morphology between

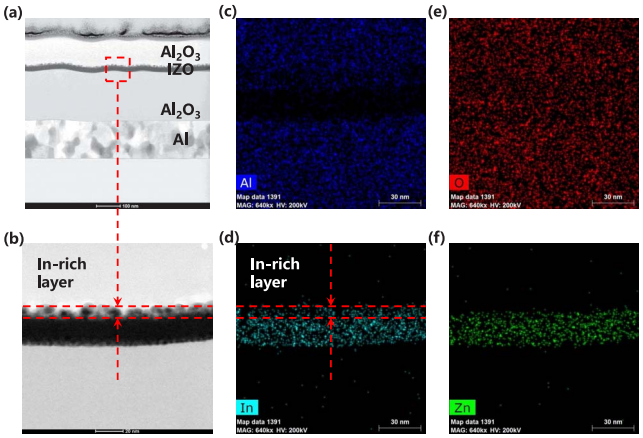

FIGURE 3. (a) Cross-sectional STEM image of passivated Cu-contact TFT; (b) Magnified STEM image of the interface between a-IZO and Al_2O_3 PVL; (c-f) Corresponding EDS mapping images of Al, In, O and Zn elements, respectively.

the Al_2O_3 PVL and the a-IZO film was observed. We obviously note that a thin layer formed on the surface of the a-IZO film. Fig. 3(c)-(f) shows the corresponding composition distribution of Al, In, O and Zn elements, respectively. Compared interfacial morphology with elemental distribution, we find that the thin layer contains a significant amount of indium. Per above results, it is entirely reasonable to assume that the bombardment of energetic particles breaks the indium-oxygen bond during the sputtering of Al_2O_3 PVL to form the In-rich layer [16], [17]. Moreover, the In-rich layer can increase carrier concentration and act as conduction paths to lower the channel resistance. However, as the carrier concentration in the channel increased, the depletion layer capacitance also increased, which resulted in a larger SS than the device without the Al_2O_3 PVL [18].

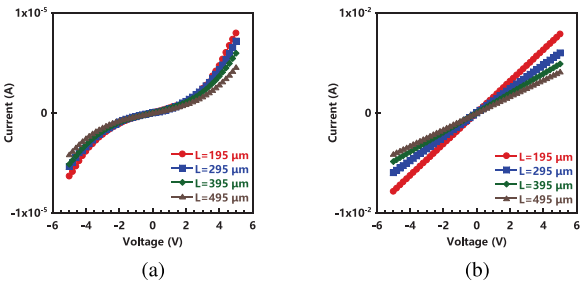

FIGURE 4. Current-voltage characteristics of passivated a-IZO film with (a) Cu and (b) Mo electrodes.

Current-voltage (I-V) characteristics of the a-IZO film with different metal electrodes were used to investigate contact properties. Fig. 4 shows the I-V characteristics of a-IZO films with Cu and Mo S/D. We can see that the Mo electrodes show perfect ohmic contact with linear curves, while the Cu electrodes exhibit regular Schottky contact. It is widely known that the chemical bonds of Cu-O form a covalent hybridized band between the O 2*p*6 and Cu 3*d*9 orbitals at the top of the valence band, resulting in p-type

properties [19]. Cu doping is introduced as acceptors or acceptor-like traps in ZnO [20] and $InGaZnO_x$ [21] films to suppress the carrier concentration. In this case, a decrease of the carrier concentration beneath the contact area due to Cu diffusion results in a high contact potential, which makes the Cu-contact behave like a Schottky contact.

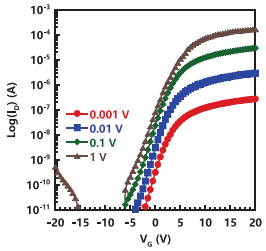

FIGURE 5. Transfer characteristics of the passivated Cu-contact a-IZO TFT at different drain voltage.

From these results, the operating mechanism of the high mobility TFT can be attributed to the formation of the Schottky contact. As mentioned by previous researchers [22], the Schottky contact induces high barrier at both ends of the S and D electrodes can prevent electrons from moving freely through the channel at a high negative gate voltage, thereby suppressing the leakage current of the TFT, even if the active layer is highly conductive. Transfer characteristics of passivated Cu-contact TFT under different drain voltage (V_D) was further conducted to understand the effect of the Schottky-barrier, as shown in fig. 5. We can find that the turn-on voltage (V_{on}) of the TFT exhibits a positive shift as V_D decreases. This phenomenon indicates that the device requires more energy to pass through the Schottky barrier, so a higher V_{on} is needed to turn on the TFT. This conjecture is supported by the switching characteristics of the passivated Cu-contact TFT and the conductor-like behavior of the passivated Mo-contact TFT.

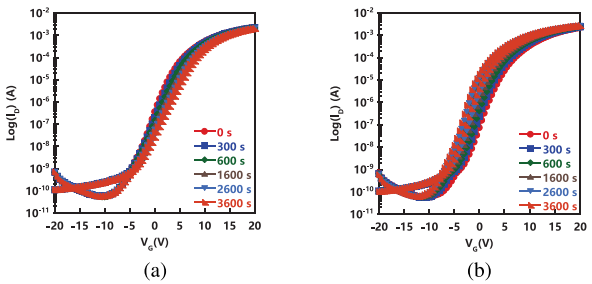

FIGURE 6. Variations of the transfer characteristics of the passivated Cu-contact TFT under (a) positive and (b) negative bias stress. $V_G = 10$ V (PBS) and -10 V (NBS), $V_D = 10$ V for 3600 s.

Ambient and bias-stress stability of the passivated Cu-contact TFT is further investigated. The TFT exhibits a superior ambient reliability that μ_{sat} as high as 409.0 cm^2/Vs is still obtained, and V_{th} varies just from 3.6 V to 3.2 V when exposed to air over 36 days. The superior ambient reliability indicates that Al_2O_3 PVL can protect the TFT from ambient influence efficiently. However, the bias-stress stability of the passivated Cu-contact TFT is not ideal. Fig. 6 displays the transfer curves of the passivated Cu-contact TFT under stress. The bias stress conditions are as follows: $V_G = 10$ V for positive bias stress (PBS), $V_G = -10$ V for negative bias stress (NBS), $V_D = 10$ V during stress. The TFT exhibits V_{th} shift of 2.4 V for PBS and −4.6 V for NBS at a stress of 3600 s. It is well known that the gate bias instability can be attributed to the charge trapping or states creation in or near the active layer. When PBS is applied, trap states are generated in the channel, resulting in more carriers trapping and a positive V_{th} shift. While NBS is applied, the deep level oxygen vacancies will release excess electrons, leading to a negative V_{th} shift [23], [24]. Therefore, the instability should be attributed to the creation of defects and the deep level oxygen vacancies.

IV. CONCLUSION

In summary, we have successfully fabricated a high mobility a-IZO TFT based on Cu S/D with Al_2O_3 PVL. The sputtering of Al_2O_3 induced a highly conductive channel of a-IZO by breaking the indium-oxygen bond to generate an In-rich layer. Moreover, a Schottky contact formed at the interface between Cu S/D and a-IZO channel, which resulted from the Cu diffusion during the thermal treatment. Thus, the TFT with Cu S/D exhibited proper switching operations with saturation mobility up to 412.7 cm^2/Vs. The results of this study suggest an efficient method fabricate high mobility metal oxide TFT based on Cu S/D.

REFERENCES

[1] Y. Liao *et al.*, "Development of a 120 hz 110' ultra-high-definition a-Si liquid crystal display panel," *J. Inf. Display*, vol. 15, no. 2, pp. 77–80, 2014, doi: 10.1080/15980316.2014.907214.

[2] N. Gong *et al.*, "58.2: Distinguished paper: Implementation of 240hz 55-inch ultra definition LCD driven by a-IGZO semiconductor TFT with copper signal lines," in *SID Symp. Dig. Tech. Papers*, vol. 43, 2012, pp. 784–787, doi: 10.1002/j.2168-0159.2012.tb05902.x.

[3] L. Zhou *et al.*, "Power consumption model for AMOLED display panel based on 2T-1C pixel circuit," *J. Display Technol.*, vol. 12, no. 10, pp. 1064–1069, Oct. 2016, doi: 10.1109/JDT.2016.2583665.

[4] M. Zhao *et al.*, "Method for fabricating amorphous indium-zinc-oxide thin-film transistors with copper source and drain electrodes," *IEEE Electron Device Lett.*, vol. 36, no. 4, pp. 342–344, Apr. 2015, doi: 10.1109/LED.2015.2400632.

[5] S. Hu *et al.*, "Effect of post treatment for Cu-Cr source/drain electrodes on a-IGZO TFTs," *Materials*, vol. 9, no. 8, p. 623, 2016, doi: 10.3390/ma9080623.

[6] K. Nomura *et al.*, "Room-temperature fabrication of transparent flexible thin-film transistors using amorphous oxide semiconductors," *Nature*, vol. 432, no. 7016, pp. 488–492, 2004, doi: 10.1038/nature03090.

[7] E. Fortunato *et al.*, "Amorphous IZO TTFTS with saturation mobilities exceeding 100 cm^2/Vs," *Physica Status Solidi Rapid Res. Lett.*, vol. 1, no. 1, pp. R34–R36, 2007, doi: 10.1002/pssr.200600049.

[8] H.-W. Zan, C.-C. Yeh, H.-F. Meng, C.-C. Tsai, and L.-H. Chen, "Achieving high field-effect mobility in amorphous indium-gallium-zinc oxide by capping a strong reduction layer," *Adv. Mater.*, vol. 24, no. 26, pp. 3509–3514, 2012, doi: 10.1002/adma.201200683.

[9] J. C. Park, H.-N. Lee, and S. Im, "Self-aligned top-gate amorphous indium zinc oxide thin-film transistors exceeding low-temperature poly-Si transistor performance," *ACS Appl. Mater. Interfaces*, vol. 5, no. 15, pp. 6990–6995, 2013, doi: 10.1021/am401128p.

[10] J. Jang *et al.*, "Transparent high-performance thin film transistors from solution-processed SnO_2ZrO_2 gel-like precursors," *Adv. Mater.*, vol. 25, no. 7, pp. 1042–1047, 2013, doi: 10.1002/adma.201202997.

[11] D. Luo *et al.*, "Role of rare earth ions in anodic gate dielectrics for indium-zinc-oxide thin-film transistors," *J. Electrochem. Soc.*, vol. 159, no. 5, pp. H502–H506, 2012, doi: 10.1149/2.jes038205.
[12] E. Fortunato, P. Barquinha, and R. Martins, "Oxide semiconductor thin-film transistors: A review of recent advances," *Adv. Mater.*, vol. 24, no. 22, pp. 2945–2986, 2012, doi: 10.1002/adma.201103228.
[13] J.-R. Yim *et al.*, "Effects of metal electrode on the electrical performance of amorphous In–Ga–Zn–O thin film transistor," *Jpn J. Appl. Phys.*, vol. 51, no. 1R, 2011, Art. no. 011401, doi: 10.1143/JJAP.51.011401.
[14] J. Park *et al.*, "Source/drain series-resistance effects in amorphous gallium–indium zinc-oxide thin film transistors," *IEEE Electron Device Lett.*, vol. 29, no. 8, pp. 879–881, Aug. 2008, doi: 10.1109/LED.2008.2000815.
[15] W.-S. Kim *et al.*, "An investigation of contact resistance between metal electrodes and amorphous gallium–indium–zinc oxide (a-GIZO) thin-film transistors," *Thin Solid Films*, vol. 518, no. 22, pp. 6357–6360, Sep. 2010, doi: 10.1016/j.tsf.2010.02.044.
[16] G. Jang *et al.*, "Device characteristics of amorphous indium-gallium-zinc-oxide channel capped with silicon oxide passivation layers," *Mater. Sci. Semicond. Process.*, vol. 49, pp. 34–39, Jul. 2016, doi: 10.1016/j.mssp.2016.03.020.
[17] J.-S. Park, J. K. Jeong, Y.-G. Mo, H. D. Kim, and S.-I. Kim, "Improvements in the device characteristics of amorphous indium gallium zinc oxide thin-film transistors by ar plasma treatment," *Appl. Phys. Lett.*, vol. 90, no. 26, 2007, Art. no. 262106, doi: 10.1063/1.2753107.
[18] S. D. Brotherton, *Introduction to Thin Film Transistors*. Heidelberg: Springer, 2013, doi: 10.1007/978-3-319-00002-2.
[19] S. Nandy, A. Banerjee, E. Fortunato, and R. Martins, "A review on Cu2o and Cui-based p-type semiconducting transparent oxide materials: Promising candidates for new generation oxide based electronics," *Rev. Adv. Sci. Eng.*, vol. 2, no. 4, pp. 273–304, 2013, doi: 10.1166/rase.2013.1045.
[20] Y. Kanai, "Admittance spectroscopy of Cu-doped Zno crystals," *Jpn J. Appl. Phys.*, vol. 30, no. 4, p. 703, 1991, doi: 10.1143/JJAP.30.703.
[21] S. I. Kim *et al.*, "High reliable and manufacturable gallium indium zinc oxide thin-film transistors using the double layers as an active layer," *J. Electrochem. Soc.*, vol. 156, no. 3, pp. H184–H187, 2009, doi: 10.1149/1.3060129.
[22] T. T. Trinh, K. Jang, V. A. Dao, and J. Yi, "Effect of high conductivity amorphous InGaZno active layer on the field effect mobility improvement of thin film transistors," *J. Appl. Phys.*, vol. 116, no. 21, 2014, Art. no. 214504, doi: 10.1063/1.4902856.
[23] L.-C. Liu, J.-S. Chen, and J.-S. Jeng, "Role of oxygen vacancies on the bias illumination stress stability of solution-processed zinc tin oxide thin film transistors," *Appl. Phys. Lett.*, vol. 105, no. 2, 2014, Art. no. 023509, doi: 10.1063/1.4890579.
[24] R. Z. Wang, S. L. Wu, X. Y. Li, and J. T. Zhang, "The electrical performance and gate bias stability of an amorphous InGaZno thin-film transistor with HfO_2 high-K dielectrics," *Solid-State Electron.*, vol. 133, pp. 6–9, Jul. 2017, doi: 10.1016/j.sse.2017.04.004.

SHIBEN HU received the B.S. degree in material physics from the Wuhan Institute of Technology in 2009. He is currently pursuing the Ph.D. degree in material physics and chemistry with the South China University of Technology, Guangzhou, China. His research interests currently include oxide semiconductor materials, thin-film transistors, and copper interconnection.

HONGLONG NING, photograph and biography not available at the time of publication.

KUANKUAN LU, photograph and biography not available at the time of publication.

ZHIQIANG FANG, photograph and biography not available at the time of publication.

RUIQIANG TAO, photograph and biography not available at the time of publication.

RIHUI YAO, photograph and biography not available at the time of publication.

JIANHUA ZOU, photograph and biography not available at the time of publication.

MIAO XU, photograph and biography not available at the time of publication.

LEI WANG, photograph and biography not available at the time of publication.

JUNBIAO PENG, photograph and biography not available at the time of publication.